Arab J Sci Eng (2016) 41:2453–2464
DOI 10.1007/s13369-015-1877-5

RESEARCH ARTICLE - CHEMICAL ENGINEERING

Batch Adsorption Studies on the Removal of Acid Blue 25 from Aqueous Solution Using *Azolla pinnata* and Soya Bean Waste

Muhammad Raziq Rahimi Kooh[1] · **Muhammad Khairud Dahri**[1] · **Linda B. L. Lim**[1] · **Lee Hoon Lim**[1]

Received: 30 April 2015 / Accepted: 5 October 2015 / Published online: 26 October 2015

Abstract *Azolla pinnata* (AP) and soya bean waste (SBW) were studied for their potentials to remove hazardous dye, acid blue 25 (AB25), from aqueous solution in a batch adsorption process. Various parameters such as pH, contact time, concentration and temperature were studied. The optimum pH was found to be at pH 2.0, and short duration of contact time at 180 min was sufficient to attain equilibrium. The experimental data were fitted to three different isotherm models, and the adsorption was best described by the Langmuir isotherm model. The maximum monolayer capacities were estimated to be 38.3 and 50.5 mg g^{-1} for SBW and AP, respectively. Kinetics studies showed that the adsorption system for both adsorbents follow pseudo-second-order model. Weber–Morris model showed that intraparticle diffusion is not the rate-limiting step, while Boyd model suggested that film diffusion may be the controlling mechanism for both adsorbent. The adsorption processes were found to be thermodynamically feasible. AP-AB25 system is endothermic in nature, while SBW-AB25 is exothermic. Regeneration experiment showed that NaOH is effective at regenerating the spent adsorbent, where at fifth cycle, the adsorption capacities of AP and SBW were comparable to the unspent adsorbents. All of these discoveries highlighted the potential of both AP and SBW as effective adsorbents for removal of AB25.

Keywords Acid blue 25 · Adsorption · Langmuir · Kinetics · Thermodynamics · Soya bean · *Azolla pinnata*

✉ Muhammad Raziq Rahimi Kooh
chernyuan@hotmail.com

Muhammad Khairud Dahri
kiddri86@hotmail.com

Linda B. L. Lim
linda.lim@ubd.edu.bn

Lee Hoon Lim
leehoon.lim@ubd.edu.bn

[1] Faculty of Science, Universiti Brunei Darussalam, Jalan Tungku Link, Pengkalan Gadong, Bandar Seri Begawan BE 1410, Brunei Darussalam

1 Introduction

Synthetic dye industry has become prevalent and important in modern lifestyle, and the uses of dyes have extended from textile dyeing, printing, and leather colouring to food colouring agents. The usefulness of dye is not limited to colouring purposes, as some dyes with antifungal and antiseptic properties are used to disinfect water in aquaculture as well as preservatives in animal feeds [1,2].

Dye effluents entering water bodies can lead to severe ecological problems and cause destruction of aquatic ecosystem, and extend the damages to agriculture and aquaculture areas. Some synthetic dyes are toxic, visible at low concentration and resistant to fading. Low dissolved oxygen level of water bodies is usually associated with dye wastewater as the reduction in sunlight penetrating the water reduces photosynthesis activity of aquatic plants and algae [3]. The dye residues can also bio-accumulate in fish and other fauna and transfer to higher food chain [1]. Discharging dye wastewater into the conventional sewage treatment leads to higher cost of treatment. This is because sewerage system is dependent on biological processes, and studies showed that sewage treatment is ineffective to treat dye wastewater due to the stability of synthetic dyes and its antimicrobial nature [4]. These reasons call for a need of cheap and efficient dye wastewater management from responsible industries.

There are many methods of dye wastewater treatment, and the advantages and disadvantages are widely covered in liter-

ature [5]. Some examples of wastewater treatment include the use of oxidising/reducing agents, Fenton's reagent, electrochemical decomposition, membrane filtration, ion-exchange technologies and adsorption method.

Adsorption method is much favoured due to the low input cost and the simple design. Moreover, adsorption method is more practical and can be easily picked up by small companies as such method is more affordable. The simplicity nature of the treatment method does not require the possession of advanced knowledge in order to treat the wastewater, thus bypassing the knowledge barrier of semi-skilled technicians.

The choice of adsorbents ranged from abundant plant materials such as casuarina [6], invasive weeds such as water fern [7,8], soil materials such as peat and diatomite [9,10], carbonaceous materials such as activated carbon [11], and agricultural wastes such as walnut shell [12], shrimp shell [13], and fruit peels (e.g. peels from tarap, breadnut and dragonfruit) [14–16]. For example, report has shown that natural low-cost adsorbents such as peat was able to remove brilliant green dye with high maximum adsorption capacity of 265 mg g^{-1} [17], while the use of bacteria such as Bacillus cereus RC-1 was successfully used in bioremediation of aqueous solution containing Cd(II) [18].

This study aimed to investigate the potential of two adsorbents, *Azolla pinnata* (AP) and soya bean waste (SBW), to remove anionic dye acid blue 25 (AB25) by the adsorption method. Both the adsorbents were chosen due to their abundance and availability around the world. AP is a water fern that possesses proliferous growth ability and can cover a stagnant water surface within a short duration of time and is found in most Asian countries, while soya bean is one of the major global cash crops where the waste is usually in huge abundance. Another reason of choosing AP is due to limited adsorption studies on using non-living AP samples by adsorption. Previous reported works of using AP by adsorption method include removal of Cd [19], methyl violet 2B and malachite green [7,8], whereas there are more studies conducted by using living samples to remove heavy metal pollutants such as Ar, Hg, Cd, Zn and Pb [20–22] by phytoremediation method.

Acid blue 25 belongs to an anthraquinone dye class which is the second most important commercial dye class after azo dyes. It is mainly used for dying wool, polyamide, leather, detergent, wood, fur, cosmetic, ink and biological stain [23]. However, AB25 can cause irritation to the eye, respiratory system and skin. AB25 was reported to be highly toxic to fish, with LC_{50} for *Pimephales promelas* (fathead minnow) at 12 mg L^{-1} [24].

The objectives of this study include the various characterisations of the adsorbents, dye removal at different dye concentration, contact time and solution pH. Adsorption isotherm, kinetics, thermodynamics and regeneration experiment were also studied.

2 Materials and Methods

2.1 Preparation of Adsorbents and Adsorbate

AP was obtained from the Department of Agriculture, Ministry of Industrial and Primary Resources, Brunei Darussalam, and SBW was obtained from local tofu shop. All the adsorbent samples were washed with distilled water and sonicated for 30 min. Washed water was discarded, and samples were dried in oven at 70 °C for 48 h. Dried adsorbents were ground with mortar and pestle and sieved to size below 355 μm. The dried and sieved samples were kept in desiccators.

AB25 (chemical formula of sodium salt, $C_{20}H_{13}N_2NaO_5S$, and IUPAC name, sodium;1-amino-4-anilino-9,10-dioxoanthracene-2-sulphonate, M_r 416.38 g mol^{-1}) of 45 % dye purity was purchased from Sigma-Aldrich Corporation and used as received. A 500 mg L^{-1} AB25 stock solution was prepared by dissolving desired amount of dye powder in distilled water, and serial dilutions were carried out to obtain lower dye concentrations.

2.2 Characterisation of Adsorbents

The elemental CHNS compositions of the adsorbents were determined using a Thermo Scientific Flash 2000 Organic Elemental Analyzer CHNS/O. The elemental analyses were determined by using X-ray fluorescence (XRF) spectrophotometer (PANalytical $Axios^{max}$). The sampling disc was prepared by using 0.12 g of the adsorbent and compressed under 10 tonne pressure.

Fourier transform infrared (FTIR) spectra of the adsorbents were obtained by the KBr disc method using a Shimadzu Model IRPrestige-21 spectrophotometer. KBr discs were made by compressing 20 mg of samples with 200 mg of spectroscopy grade KBr under 10 tonne pressure.

Morphological analysis of adsorbent's surface was done using Tescan Vega XMU scanning electron microscope (SEM). Dried adsorbent was mounted on carbon conducting adhesive tape and sputter coated with gold using SPI-MODULE^{TM} Sputter Coater for 60 s. SEM images were taken at 500× magnification.

The point of zero charge (pH_{pzc}) of the adsorbents were determined by the salt addition method using 0.1 mol L^{-1} KNO_3 solutions [25]. The pH of the KNO_3 solutions were adjusted with 0.1 mol L^{-1} HNO_3 and NaOH to initial pH of 2.0–10.0. The pH was measured using a Thermo Scientific Orion 2 Star pH Benchtop meter. 0.04 g of respective samples were added to 20 mL of pH-adjusted KNO_3 and agitated for 24 h at 250 rpm using a Stuart orbital shaker, and the final pH was measured. The pH difference, ΔpH (final pH–initial pH) versus initial pH was plotted to determine the pH_{pzc}.

2.3 Batch Adsorption Procedures

2.3.1 Basic Procedures

All experiments were carried out in duplicates at the adsorbent dosage of 0.04 g/20 mL dye solution using 150-mL Erlenmeyer flasks and agitated at 250 rpm. The dye filtrates were analysed using a Shimadzu UV-1601PC UV–visible spectrophotometer at wavelength 597 nm.

The amount of adsorbate in adsorbent at equilibrium, q_e (mg g^{-1}), is calculated using the following equation:

$$q_e = \frac{(C_i - C_e)\,V}{m} \tag{1}$$

where C_i is the initial dye concentration (mg L^{-1}), C_e is the dye concentration at equilibrium (mg L^{-1}), V is the volume of dye solution used (L) and m is the mass of adsorbent used (g).

The percentage removal is calculated by the following equation:

$$\text{Percentage removal} = \frac{(C_i - C_e) \times 100\,\%}{C_i} \tag{2}$$

2.3.2 Effect of pH and Contact Time

Effect of pH was studied from pH 2.0 to 8.0. Effect of contact time was done by agitating the adsorbent with 100 mg L^{-1} AB25, and the filtrates were collected at predetermined time intervals (5–240 min). The experiment was repeated for 200, 300 and 400 mg L^{-1}. Four kinetics models (pseudo-first-order [26], pseudo-second-order [27], Weber–Morris intraparticle diffusion [28] and Boyd [29] models) were used for characterising the kinetics data.

The pseudo-first-order is typically expressed as:

$$\log (q_e - q_t) = \log q_e - \frac{t}{2.303} k_1 \tag{3}$$

where q_t is the amount of adsorbate adsorbed per gram of adsorbent (mg g^{-1}) at time t, k_1 is the pseudo-first-order rate constant (min^{-1}) and t is the time shaken (min).

The pseudo-second-order is commonly expressed as:

$$\frac{t}{q_t} = \frac{1}{q_e^2 k_2} + \frac{t}{q_e} \tag{4}$$

where k_2 is pseudo-second-order rate constant (g mg^{-1} min^{-1}).

The Weber–Morris intraparticle diffusion model is expressed as:

$$q_t = k_3 t^{1/2} + C \tag{5}$$

where k_3 is the intraparticle diffusion rate constant (mg g^{-1} $min^{-1/2}$) and C is the intercept.

The Boyd model is expressed as:

$$B_t = -0.4977 - \ln (1 - F) \tag{6}$$

where F is equivalent to $\frac{q_t}{q_e}$ and B_t is mathematical function of F.

The rate constant and parameters of the pseudo-first-order, pseudo-second-order, Weber–Morris intraparticle diffusion and Boyd models were obtained from the linear plots of $\ln (q_e - q_t)$ versus t, $\frac{t}{q_t}$ versus t, q_t versus $t^{1/2}$ and B_t versus t, respectively.

2.3.3 Effect of Initial Concentration

The effect of initial concentration was carried out between the C_i ranged from 40 to 500 mg L^{-1} and this experiment was repeated under different temperature (35, 45, 55 and 65 °C) to investigate the effect of temperature on the adsorption process. Three isotherm models were used for modelling the adsorption data: Langmuir [30], Freundlich [31] and Dubinin–Radushkevich (D–R) [32].

The Langmuir isotherm is one of the commonly used isotherm model, which assumes monolayer coverage of adsorbate molecules onto the adsorbent surface.

The Langmuir equation is generally expressed as:

$$\frac{C_e}{q_e} = \frac{1}{k_L q_m} + \frac{C_e}{q_m} \tag{7}$$

where q_m is the maximum monolayer adsorption capacity of the adsorbent (mg g^{-1}), and k_L is the Langmuir adsorption constant (L mg^{-1}) which is related to the free energy of adsorption.

The separation factor (R_L) is a dimensionless constant which is an essential characteristic of the Langmuir model. The equation of R_L is expressed as:

$$R_L = \frac{1}{(1 + k_L C_o)} \tag{8}$$

where C_o (mg L^{-1}) is the highest initial dye concentration (C_o = 500 mg L^{-1}). R_L indicates if the isotherm is unfavourable ($R_L > 1$), linear ($R_L = 1$), favourable ($0 < R_L < 1$), or irreversible ($R_L = 0$).

The Freundlich isotherm model assumes multilayer coverage of adsorbate onto the adsorbent surface, and the equation is typically expressed as:

$$\ln q_e = \frac{1}{n_F} \ln C_e + \ln k_F \tag{9}$$

where k_F ($mg^{1-1/n}\,L^{1/n}\,g^{-1}$) is the adsorption capacity of the adsorbent and n_F (Freundlich constant) indicates the favourability of the adsorption process. The adsorption process is considered favourable if $1 < n_F < 10$.

D–R isotherm assumes no homogenous surface of the adsorbent and is temperature dependent. The equation is as follows:

$$\ln q_e = \ln q_m - k_{DR}\varepsilon^2 \tag{10}$$

where q_m is the saturation capacity (mg g^{-1}), k_{DR} is a D–R constant ($mol^2\,kJ^{-2}$) and ε is the D–R isotherm constant which is also known as the Polanyi potential.

The D–R isotherm constant, ε, is expressed as:

$$\varepsilon = RT\ln\left[1 + \frac{1}{C_e}\right] \tag{11}$$

where R is the gas constant (8.314×10^{-3} kJ $mol^{-1}\,K^{-1}$) and T is temperature (K).

The mean free energy, E(kJ mol^{-1}), of the sorption per molecule of adsorbate is obtained from k_{DR}, and the equation is expressed as:

$$E = \frac{1}{\sqrt{2k_{DR}}} \tag{12}$$

The parameters of the isotherm models Langmuir, Freundlich and D-R isotherm were obtained from the linear plot of C_e/q_e versus C_e, $\ln q_e$ versus $\ln C_e$ and $\ln q_e$ versus ε^2, respectively.

2.4 Thermodynamics Study

The thermodynamics parameters were studied from temperature 25 °C to 65 °C.

The Van Hoff equation is used in the thermodynamics studies, and it is expressed as:

$$\Delta G^o = \Delta H^o - T\Delta S^o \tag{13}$$

where ΔG^o is the Gibbs free energy, ΔH^o is the change in enthalpy, ΔS^o is the change in entropy and T is the temperature (K)

The Gibbs energy is expressed as:

$$\Delta G^o = -RT\ln k \tag{14}$$

$$k = \frac{C_s}{C_e} \tag{15}$$

where k is the distribution coefficient for adsorption, C_s is the concentration of dye adsorbed by the adsorbent at equilibrium (mg L^{-1}), C_e is the concentration of dye remains in solution at equilibrium (mg L^{-1}) and R is the gas constant (J $mol^{-1}\,K^{-1}$).

Substitution of equation 13 into equation 14 yields the following equation:

$$\ln k = \frac{\Delta S^o}{R} - \frac{\Delta H^o}{RT} \tag{16}$$

The linear plot of $\ln k$ versus T^{-1} was used for obtaining the thermodynamics parameters.

2.5 Regeneration Experiment

The regeneration experiment was investigated with three solvents (distilled water, 0.1 mol L^{-1} HNO_3 and 0.1 mol L^{-1} NaOH). The detailed procedure of regeneration experiment was described in our previous work [12]. Briefly, both adsorbents were treated with 100 mg L^{-1} AB25 of adsorbent dosage 2.0 g L^{-1}. Dye-treated adsorbent was agitated in a beaker of distilled water for several times until little desorption of dye occurred. Adsorbent was filtered and dried at 70 °C for 24 h, for the next cycle. For acidic and basic washing, dye-treated adsorbents were initially agitated in respective solvents for 30 min and followed by repeated distilled water washing until the washed solution become near neutral. The regeneration experiment was repeated up to the fifth cycle.

3 Results and Discussion

3.1 Characterisation of Adsorbent

The CHNS compositions of AP were determined to be at average of 44.18 % C, 6.27 % H, 4.01 % N and 0.20 % S, whereas SBW contained 44.14 % C, 6.62 % H, 3.11 % N and 0.07 % S, while the result of XRF elemental analysis is summarised in Table 1.

3.2 FTIR

FTIR analyses of AP and SBW before and after treatment with AB25 are illustrated in Fig. 1. Both AP and SBW share similar pattern of observed bands in the spectra. Broadbands at 3340–3360 cm^{-1} are attributed to −OH (hydroxyl & carboxyl) and −NH groups. Aliphatic C−H stretching bands are found at around 2920 cm^{-1}. The band at 1650 cm^{-1} may be assigned to primary −NH bending vibration. Band at 1741 cm^{-1} is only present only in SBW is the stretching vibration of C=O groups. C–N stretching for aromatic amine is found at around 1246 cm^{-1}, while bands at around 1070 cm^{-1} can be assigned to stretching vibration of C–OH of alcoholic and carboxylic acid. After AB25 treatment, the bands at 3347 cm^{-1} (AP) and 3358 cm^{-1} (SBW) were shifted to 3363 and 3373 cm^{-1}, respectively. Bands that represent

Table 1 XRF elemental analysis of untreated and dye-treated adsorbents

Elements	Normalised percentage (%)	
	Untreated AP	Untreated SBW
Al	0.45	1.33
Mn	0.49	ND
Ru	0.91	2.40
Si	1.23	0.09
P	2.48	1.99
S	3.59	2.39
Mg	3.66	1.64
Na	4.38	0.23
Fe	6.58	8.20
Cl	8.65	0.48
Ca	12.31	13.23
Zn	12.39	20.42
K	14.39	20.31
O	28.47	27.30

ND not detected

amine group in AP (1650 and 1244 cm^{-1}) and SBW (1651 and 1246 cm^{-1}) were also shifted, which indicate that the amine group may be involved in the interaction with AB25. Finally, bands at 1076 cm^{-1} (AP) and 1068 cm^{-1} (SBW) that represent the alcoholic and carboxylic acid C–OH were both shifted to 1022 cm^{-1}. This suggests that the amine, carboxyl and hydroxyl group may be involved in the interaction with AB25, which is in agreement with result as obtained by Hanafiah et al. [33], who proposed the following equations showing possible electrostatic interactions in a medium under acidic conditions.

$$RCOOH_2^+ + RSO_3^- \leftrightharpoons RCOOH_2^+ \cdots {}^-O_3SR \quad (17)$$

$$ROH_{2+} + RSO_3^- \leftrightharpoons ROH_2^+ \cdots {}^-O_3SR \quad (18)$$

$$RNH_3^+ + RSO_3^- \leftrightharpoons RHN_3^+ \cdots {}^-O_3SR \quad (19)$$

Equations 17–19 show that the suggested electrostatic attractions between the various positively charged functional groups on the adsorbent surface and the sulphonate group of AB25 at pH 2.

3.3 SEM Images

Surface morphology of the adsorbent was analysed with SEM. Figure 2a, c displayed the rough surface of both AP and SBW adsorbents, respectively, while Fig. 2b, d showed the AB25-treated adsorbents. It was concluded that there were no obvious changes in the surface morphology of the adsorbent after exposure to dye.

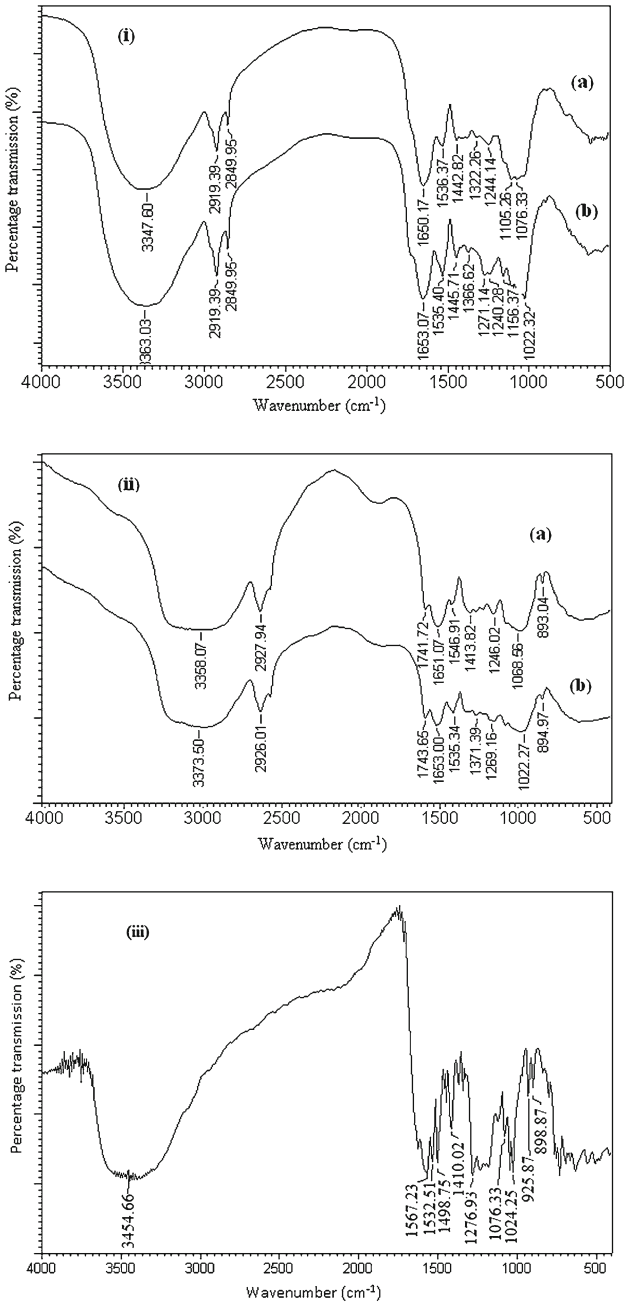

Fig. 1 The FTIR spectra of (**i**) adsorbent AP, (**ii**) adsorbent SBW and (**iii**) AB25 dye; while (*a*) is untreated adsorbent and (*b*) AB25-treated adsorbent

3.4 Effect of pH

Effect of pH is one of the essential studies in adsorption process because pH of the aqueous solution (pH_{aq}) influences mainly the electrostatic attraction between the adsorbent and the dye molecule.

The pH_{pzc} of AP and SBW were found to be at 6.6 and 4.1, respectively, at adsorbent dosage of 2.0 g L^{-1}. According to the concept of point of zero charge, if $pH_{aq} < pH_{pzc}$, then ad-

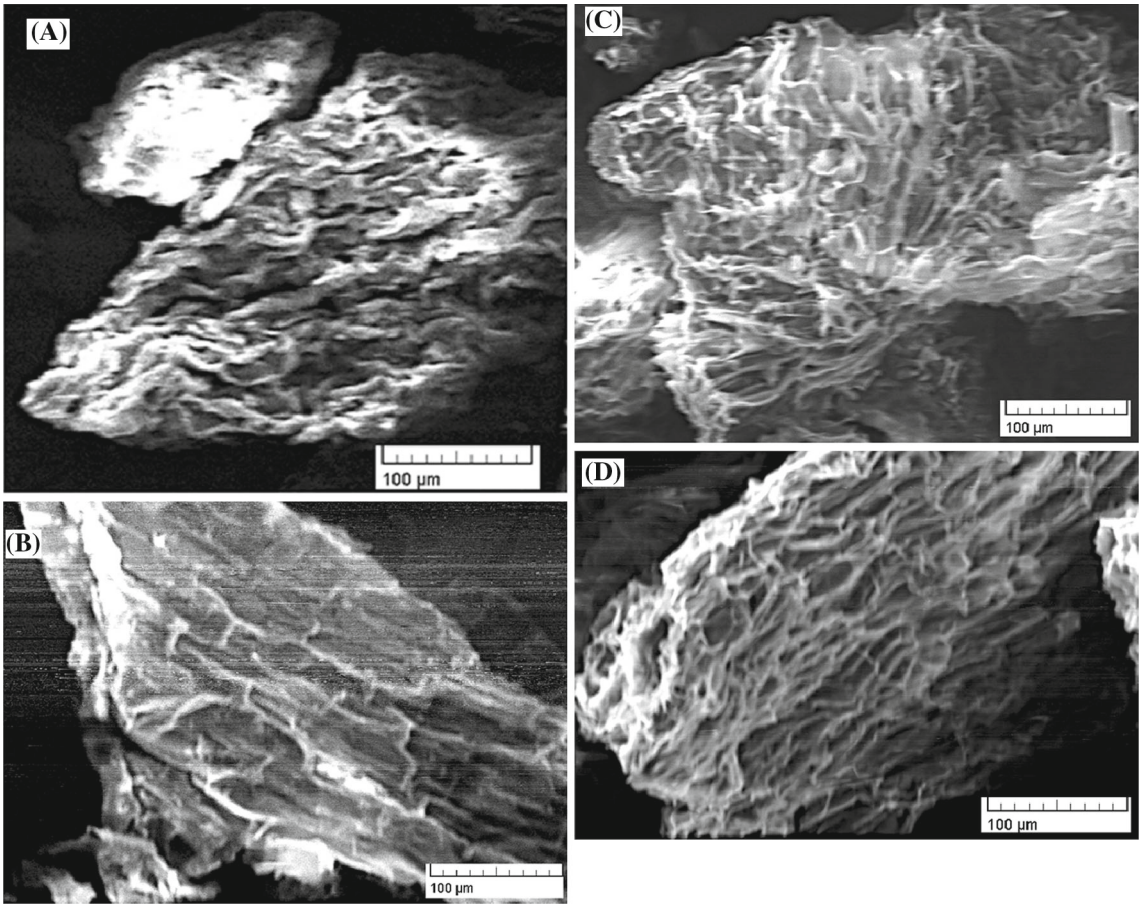

Fig. 2 SEM images of (**a**) untreated AP, (**b**) AB25-treated AP, (**c**) untreated SBW and (**d**) AB25-treated SBW

sorbent surface will be predominantly positive charged, and the opposite for $pH_{aq} > pH_{pzc}$. It can be observed in Figure 3 that the SBW is more affected by medium pH than AP. SBW showed larger drop in adsorption capacity (96.2 %), while a decrease of 73.8 % was observed for AP and this adsorbent remained unaffected above pH 4.0 and beyond. The dye uptake of both adsorbents gradually increased as the $pH_{aq} < pH_{pzc}$. This can be explained by the electrostatic attraction of anionic AB25 molecules to the predominantly positive charged surface of the adsorbent particles. Low dye uptake at high pH_{aq} is due to electrostatic repulsion between the negatively charged AB25 molecules and the predominant negatively charged adsorbent surface. The optimum dye uptakes of both adsorbents are found to be at pH 2.0, thus all experimental works were carried out at this pH.

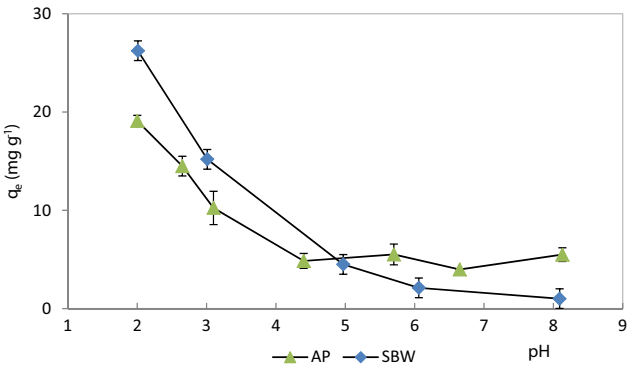

Fig. 3 Effect of pH on the adsorption of AB25 using AP and SBW

3.5 Effect of Contact Time and Kinetics Modelling

The determination of contact time between the adsorbents and the dye is essential in adsorption experiment, as it is important to know the time duration required to attain complete equilibrium. Figure 4 illustrates the effect of contact time for both adsorbents at different concentrations. Both adsorbents showed similar pattern in the experiment. Initially, the rates of adsorption were fast, up to 50 min and then gradually increase between 60 to 150 min. The rapid initial dye adsorption is due to the availability of vacant adsorption sites, which became occupied over time and eventually reached an equilibrium. When less vacant sites are available, there is an increase in repulsion force that is built up by the dye molecules in the solid

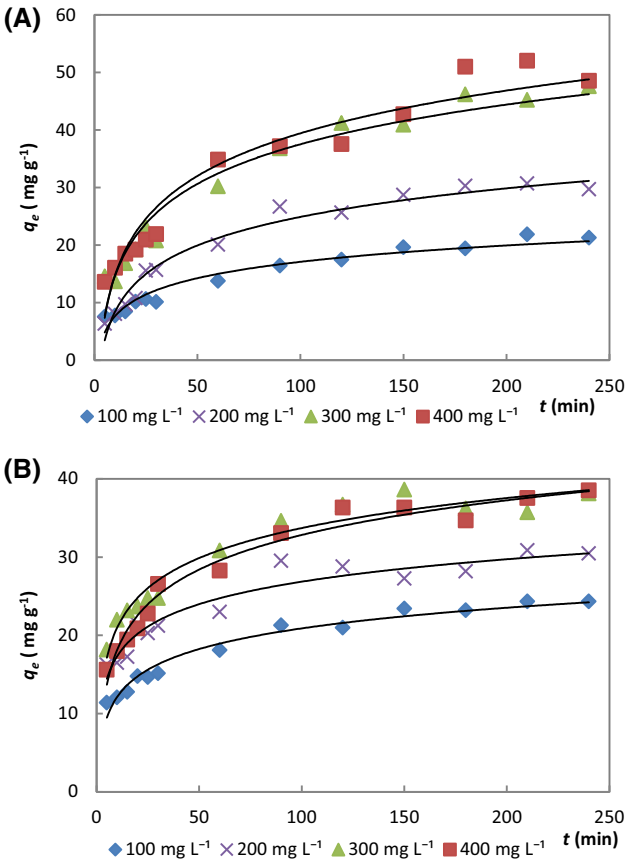

Fig. 4 Effect of contact time for (**a**) AP and (**b**) SBW at C_i 100, 200, 300, and 400 mg L^{-1}

and bulk phases, leading to slower rate of adsorption of dye [34]. Beyond 180 min, the adsorption capacities no longer increase which indicates equilibrium is reached. Therefore, all experiments were carried out at agitation time of 180 min.

To understand more about the adsorption process, these kinetics data were fitted into two kinetics models: pseudo-first-order and pseudo-second-order (linear plots not shown for brevity). The parameters of these kinetics models are summarised in Table 2.

By comparing the values of coefficient of determination, R^2, the pseudo-second-order showed better fit (AP 0.974–0.992, SBW 0.994–0.996) than the pseudo-first-order (AP 0.937–0.981, SBW 0.815–0.950). The values of the error functions, e.g. χ^2 were also lower for pseudo-second-order (AP 2–19, SBW 4–16) compared to pseudo-first-order (AP 6–81, SBW 72–171) where lower values indicate lower experimental error. Lastly, the comparison of experimental adsorption capacity ($q_{e,exp}$) to the calculated adsorption capacity ($q_{e,cal}$) was done, where pseudo-second-order showed closer values overall than the pseudo-first-order. Therefore, with consideration of the R^2, error functions and the comparison between $q_{e,exp}$ and $q_{e,cal}$, it is concluded that pseudo-second-order best represented the experimental data of both adsorbents. For both dyes, the k_2 values decrease as the concentration increases. This might be due to the higher competition for the adsorption site at high dye concentration compare to at lower dye concentration [35].

The Weber–Morris intraparticle diffusion model describes the diffusion mechanism of the adsorption processes and generally divided into three phases. The first phase is the fast external surface adsorption, followed by intraparticle diffusion phase and lastly, the slow equilibrium phase [36,37].

The parameters of the Weber–Morris model are summarised in Table 2, and the linear plots are as showed in Fig. 5. The fast external surface adsorptions were completed within 5 min and were not observed in the Weber linear plot. This behaviour was reported by other researchers [36,37].

As according to the Weber–Morris model, if the linearised plot crosses the origin, then the rate-limiting phase is the intraparticle diffusion, otherwise the diffusion is controlled by other mechanism. As the intercept of all the plots for both adsorbent-dye systems were nonzero, this showed the diffusion mechanism is not controlled by intraparticle diffusion.

The diffusion mechanism was investigated with the Boyd model. According to the Boyd model, if the linear plot of B_t versus t (plot not showed for brevity) crosses the origin, then the diffusion process is controlled by particle diffusion; otherwise, it is controlled by film diffusion. Particle diffusion is the transfer of adsorbates into the pores of adsorbent particles, while film diffusion means the transport occurred on the external surface [38]. As seen in Table 2, all the intersect for both adsorbents are nonzero, thereby suggesting that the film diffusion may be involved.

3.6 Effect of Concentration and Isotherm Modelling

The effect of concentration of AP and SBW on the removal of AB25 is summarised in Fig. 6. It can be observed that as the dye concentration increases the dye uptake by both adsorbents also increases. This increase in dye uptake is due to the increase in amount of AB25 molecules in solution which increases the interaction between the adsorbents and dye molecules. In addition, higher dye concentration provides higher driving force to overcome the mass transfer resistance of dye molecule from aqueous solution to the adsorbent [39]. However, beyond 200 mg L^{-1}, many of the graphs started to plateau; this is due to the saturation of both adsorbents' active sites by AB25 molecules. AP showed higher dye uptake at temperature of 35 and 45 °C, with only slight increase in dye uptake beyond 45 °C. This behaviour suggested that the adsorption process between AP and AB25 may be endothermic. For SBW, a slight decrease in overall dye uptake was observed at higher temperature. This behaviour suggested an exothermic reaction for the SBW-AB25 adsorption system. The detailed thermodynamics studies are included in the thermodynamics section.

Table 2 Parameters of various kinetics models for AP and SBW in removal of AB25

Parameters	AP				SBW			
Pseudo-first-order								
C_i	100	200	300	400	100	200	300	400
$q_{e,cal}$	16.4	29.1	36.2	39.1	14.1	14.1	18.2	21.8
$q_{e,exp}$	21.9	30.7	47.6	52.0	24.3	30.8	38.6	38.5
k_1	0.0126	0.0200	0.0126	0.0099	0.0151	0.0133	0.0129	0.0141
R^2	0.973	0.937	0.971	0.981	0.950	0.815	0.879	0.907
χ^2	33	6	57	81	72	132	171	124
EABS	67	23	113	160	112	178	239	196
ARE	44	15	39	48	54	63	66	59
MSDP	57	26	60	60	73	83	80	72
Pseudo-second-order								
$q_{e,cal}$	23.4	35.0	52.7	56.5	25.6	31.3	39.2	40.0
$q_{e,exp}$	21.9	30.7	47.6	52.0	24.3	30.8	38.6	38.5
k_2	0.0015	0.0008	0.0006	0.0005	0.0024	0.0027	0.0022	0.0016
R^2	0.985	0.992	0.988	0.974	0.995	0.994	0.996	0.995
χ^2	19	2	6	7	16	4	4	4
EABS	48	14	26	40	47	22	24	20
ARE	29	8	9	13	22	8	8	7
MSDP	38	12	18	19	34	16	14	14
Weber–Morris intraparticle diffusion model[a]								
k_3	1.151	2.808	3.031	3.179	1.214	1.729	2.072	2.349
C	4.6	−0.4	6.1	5.9	8.6	11.7	14.4	10.9
R^2	0.984	0.973	0.980	0.972	0.980	0.905	0.987	0.976
Boyd model[a]								
Slope	0.013	0.020	0.017	0.010	0.015	0.025	0.020	0.019
Intercept	−0.210	−0.443	−0.366	−0.212	0.049	−0.013	0.048	−0.079
R^2	0.973	0.937	0.976	0.981	0.950	0.857	0.989	0.968

[a] Calculated values only applied to initial linear region

The experimental data were fitted into various isotherm models, and the data are summarised in Table 3. Application of the isotherm models yielded favourable R^2 for both the Langmuir (AP 0.963–0.994, SBW 0.980–0.993) and Freundlich (AP 0.842–0.958, SBW 0.915–0.962) models. However, experimental data fitted poorly to the D–R model (AP 0.497–0.828, SBW 0.460–0.582). The overall error is lowest for the Freundlich model; however, the values are close to the Langmuir model, which indicate low error for both models. Thus, with the consideration of R^2 and the error functions, it is concluded that the Langmuir model best represented the adsorption data. The values of the separation factor (R_L) of both adsorbents are between 0 and 1 at concentration of 500 mg L^{-1}, which indicate that the adsorption process are favourable at high concentration. Furthermore, the values of n_F also indicated that adsorption of AB25 onto both AP and SBW is favourable.

The maximum adsorption capacity, q_m, of SBW and AP were 38.3 ± 0.2 mg g^{-1} and 50.5 ± 3.1 mg g^{-1}, respectively, and were compared to literature values summarised in Table 4. The q_m of SBW and AP are low compared to many studied adsorbents, while chemically modified adsorbents, such as wasted tea activated carbon, exhibited higher dye adsorption capacities.

3.7 Thermodynamics Studies

The adsorption thermodynamics provide useful information on energy changes of the adsorption process. The thermodynamic parameters are summarised in Table 5. The negative ΔG° showed that both dye-adsorbent systems are spontaneous in nature. The positive ΔH°(27.1 kJ mol^{-1}) of AP-AB25 system indicated an endothermic reaction, while negative ΔH°(8.24 kJ mol^{-1}) of SBW-AB25 system indicate an exothermic reaction. The positive ΔS°(91.7 J mol^{-1} K^{-1}) for AP-AB25 system indicates an increase in randomness. It was suggested by Wei et al. that the positive ΔS° is a result of "solvent-replacement" phenomenon, where the AB25 molecules need to replace the water molecules on the adsorbent surface in order to be adsorbed [41]. The negative

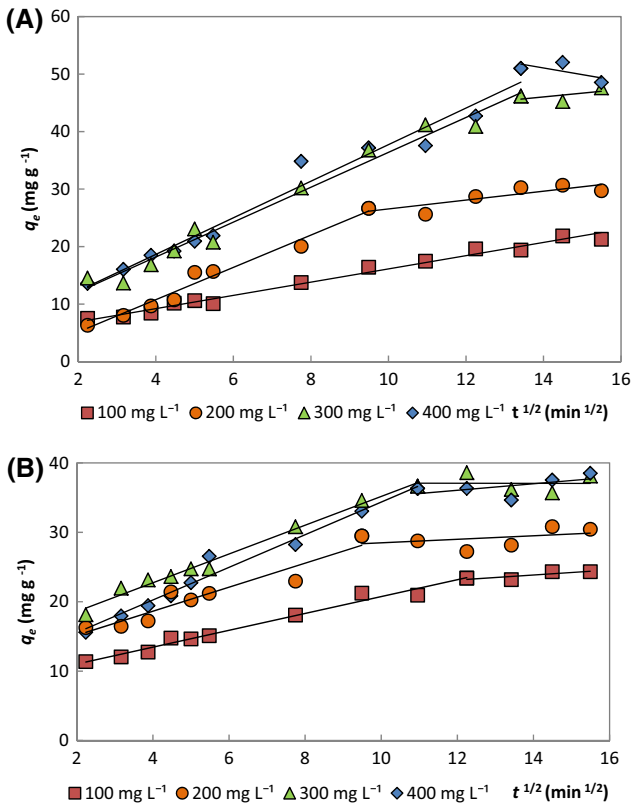

Fig. 5 The linear plots of Weber–Morris intraparticle diffusion model for (**a**) AP and (**b**) SBW

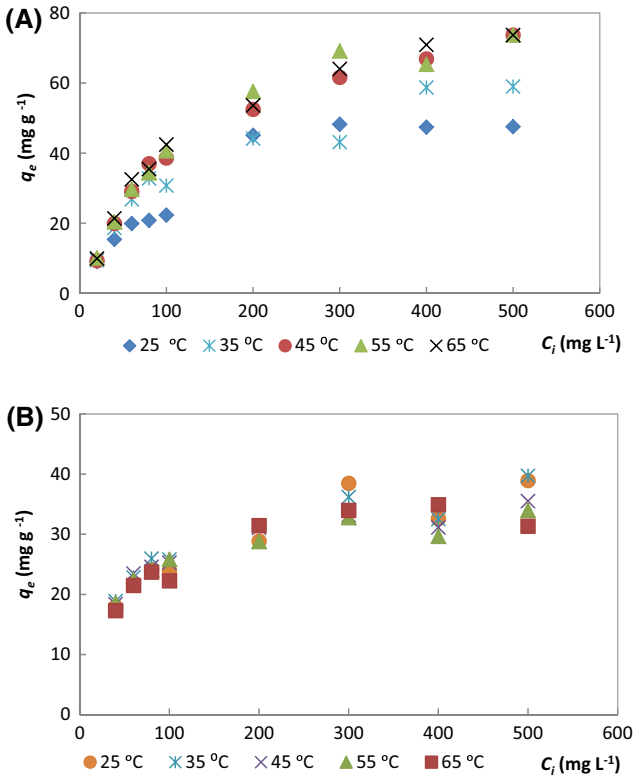

Fig. 6 Effect of initial concentration on the removal of AB25 using (**a**) AP and (**b**) SBW

$\Delta S°(-18.2\,\mathrm{J\,mol^{-1}\,K^{-1}})$ for SB-AB25 system is outweighed by the favourable negative $\Delta G°$ and large enthalpy [42].

3.8 Regeneration Experiment

Spent adsorbents must be incinerated because dumping to landfill could lead to leaching of hazardous dyes, which is an improper disposal method for hazardous waste. However, incineration also has its downside as fuel may be more costly and there is always possibility of the release of poisonous gas and other side products. Regeneration experiment explores the possibility of an alternative route to direct disposal of spent adsorbent, and the ability to reuse the spent adsorbent may minimise the total cost for adsorbent treatment. The data of regeneration experiment are summarised in Fig. 7.

Among the three studied solvents, 0.1 mol L^{-1} NaOH is the most effective in regenerating the spent adsorbent. Distilled water and acid washing regenerated less than half of the former dye uptake capacity, while NaOH regenerated more than 90 % of the first cycle. At the fifth cycle, regeneration with NaOH solvent retained the dye removal at 36.5 ± 0.5 % and 38.0 ± 0.7 % for AP and SBW, respectively, which are still considerably close to the first cycle at 41.2 ± 3.6 % and 48.6 ± 1.9 %. The effectiveness of NaOH can be explained by the high pH of the solution that leads to predominant negatively charged adsorbent surface that cause repulsion of anionic AB25 molecules.

In pH experiment, it was observed that adsorption of AB25 was unfavourable at high pH; this might explain the effectiveness of base in desorbing AB25 from the adsorbents. In such unfavourable condition, the interaction between AB25 and the adsorbent might be weakened and can be easily displaced by the OH^- present.

4 Conclusions

The potential of AP and SBW as adsorbents for the removal of AB25 was investigated in this study. Both adsorbents performed the best at pH 2.0. This proved to be advantageous as the process of dyeing with AB25 requires acidic medium. Furthermore, the uptake processes of AB25 by both adsorbents can be achieved within 180 min which is a short duration of time. Regeneration of the adsorbents carried out using 0.1 mol L^{-1} NaOH showed adsorption capacities close to that of fresh adsorbents and maintained almost the same adsorption capacities at the fifth cycle. All of these discov-

Table 3 Parameters of various isotherm models for the removal of AB25 using AP and SBW

Parameters	AP					SBW				
Langmuir isotherm										
T	25	35	45	55	65	25	35	45	55	65
q_m	50.5	59.7	70.0	72.6	73.2	38.3	38.0	34.7	33.2	33.7
k_L	0.027	0.043	0.075	0.073	0.079	0.044	0.055	0.075	0.079	0.084
R_L	0.068	0.045	0.026	0.027	0.025	0.040	0.032	0.024	0.023	0.021
R^2	0.983	0.963	0.988	0.994	0.991	0.980	0.982	0.993	0.992	0.992
χ^2	7.3	18.7	23.1	4.3	28.3	2.9	1.9	1.3	0.9	1.7
EABS	28.4	60.6	67.9	30.4	60.4	22.4	18.2	12.1	11.4	14.0
ARE	14.5	24.6	25.0	9.9	22.8	11.3	9.0	6.4	6.0	7.4
MSDP	23.6	34.7	37.3	15.8	41.4	14.9	11.9	10.1	8.3	11.7
Freundlich isotherm										
k_F	6.4	12.6	16.1	14.1	17.6	13.0	15.0	15.6	15.6	13.0
n_F	2.8	3.8	3.8	3.3	4.0	5.8	6.8	7.7	8.1	6.2
R^2	0.949	0.923	0.879	0.958	0.842	0.924	0.950	0.962	0.958	0.915
χ^2	5.1	5.0	5.4	4.4	12.7	1.3	0.7	0.4	0.4	6.8
EABS	31.7	28.7	34.9	34.7	57.4	14.4	10.2	7.5	6.4	34.7
ARE	11.1	10.2	10.8	8.6	18.1	6.4	4.5	3.6	3.0	18.2
MSDP	15.2	15.3	15.8	11.9	25.2	8.8	6.7	5.0	5.0	22.8
Dubinin–Radushkevich isotherm										
q_m	31.1	37.8	49.7	45.3	54.2	29.7	30.5	29.1	28.2	28.4
k_{DR}	2.279	0.355	0.391	0.364	0.392	3.854	1.962	1.586	1.727	3.165
E	0.468	1.188	1.131	1.173	1.129	0.360	0.505	0.561	0.538	0.397
R^2	0.497	0.661	0.828	0.637	0.816	0.460	0.499	0.582	0.562	0.510
χ^2	45.1	34.1	27.1	51.8	31.9	8.4	6.5	4.1	3.5	6.8
EABS	105.2	90.0	94.6	129.9	100.7	38.2	33.2	26.9	23.2	34.7
ARE	44.3	31.4	26.1	36.8	23.5	18.5	15.8	13.5	12.0	18.2
MSDP	54.0	43.3	32.1	48.4	31.0	24.0	21.0	17.0	16.1	22.8

Table 4 The maximum adsorption capacity of various adsorbents obtained under various conditions

Adsorbent	q_m (mg g^{-1})	pH	T (°C)	Adsorbent dosage (g L^{-1})	References
Diatomite	21.4	2	25	3.6	[10]
Base-treated *Shorea dasyphylla* sawdust	24.4	2	27	2.0	[33]
SBW	38.3	2	25	2.0	This work
AP	50.5	2	25	2.0	This work
Penicillium	90.1	3	30	1.0	[40]
Cetylpyridinium-chloride-modified penicillium	106.4	3	30	1.0	[40]
Waste tea activated carbon	203.3	7	30	1.0	[11]

Table 5 Thermodynamics parameters of AP and SBW on the removal of 100 mg L^{-1} AB25 at temperature ranged from 25 to 65 °C

Adsorbent	T (K)	ΔG° (kJ mol^{-1})	ΔH° (kJ mol^{-1})	ΔS° (J mol^{-1} K^{-1})
AP	298	−0.60	27.1	91.7
	313	−1.16		
	323	−1.23		
	333	−3.27		
	343	−4.21		
SBW	298	−2.64	−8.24	−18.2
	313	−2.74		
	323	−2.65		
	333	−2.30		
	343	−1.91		

eries along with the abundance of AP and SBW highlighted their potential as effective adsorbents for removal of AB25.

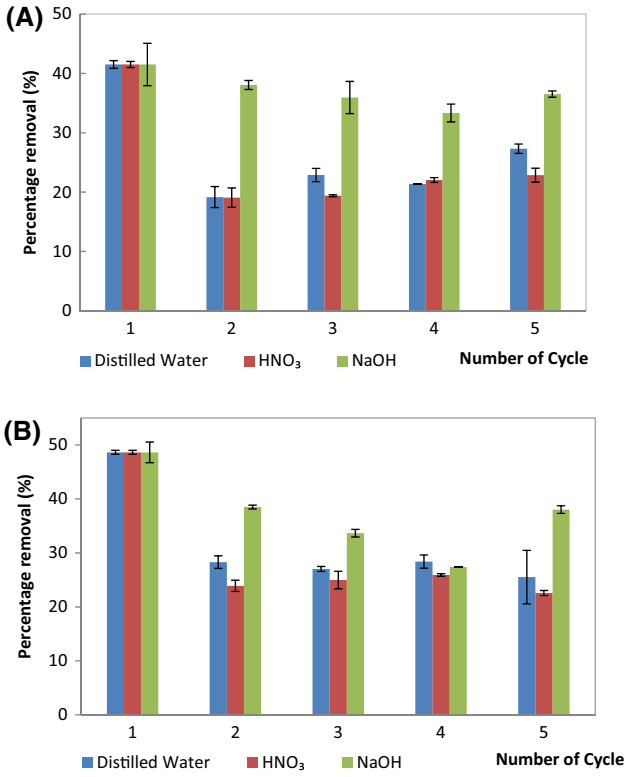

Fig. 7 Regeneration of spent adsorbents (**a**) AP and (**b**) SBW, treated with 100 mg L^{-1} AB25, using three different solvents

Acknowledgments The authors would like to thank the Government of Brunei Darussalam and the Universiti Brunei Darussalam for their support and Centre for Advanced Material and Energy Sciences (CAMES) of Universiti Brunei Darussalam for the usage of XRF machine. A special thanks to Dr H.M Thippeswamy of the Department of Agriculture (Soil and Plant Nutrition unit), Ministry of Industrial and Primary Resource, Brunei Darussalam for the provision of the *Azolla pinnata* sample.

References

1. Bajc, Z.; Jenčič, V.; Šinigoj Gačnik, K.: Elimination of malachite green residues from meat of rainbow trout and carp after water-born exposure. Aquaculture **321**, 13–16 (2011)
2. Liu, R.; Hei, W.; He, P.; Li, Z.: Simultaneous determination of fifteen illegal dyes in animal feeds and poultry products by ultra-high performance liquid chromatography tandem mass spectrometry. J. Chromatogr. B **879**, 2416–2422 (2011)
3. Sultana, Z.; Ali, M.E.; Uddin, M.S.; Haque, M.M.: Implementation of effluent treatment plants for waste water treatment. J. Environ. Prot. **4**, 301 (2013)
4. Wesenberg, D.; Kyriakides, I.; Agathos, S.N.: White-rot fungi and their enzymes for the treatment of industrial dye effluents. Biotechnol. Adv. **22**, 161–187 (2003)
5. Crini, G.: Non-conventional low-cost adsorbents for dye removal: a review. Bioresour. Technol. **97**, 1061–1085 (2006)
6. Dahri, M.K.; Kooh, M.R.R.; Lim, L.B.L.: Application of Casuarina equisetifolia needle for the removal of methylene blue and malachite green dyes from aqueous solution. Alexandria Eng. J. doi:10.1016/j.aej.2015.07.005 (2015)
7. Kooh, M.R.R.; Lim, L.B.L.; Dahri, M.K.; Lim, L.H.; Sarath Bandara, J.M.R.: *Azolla pinnata*: an efficient low cost material for removal of methyl violet 2B by using adsorption method. Waste Biomass Valoriz. **6**, 547–559 (2015)
8. Kooh, M.R.R.; Lim, L.B.L.; Lim, L.H.; Bandara, J.M.R.S.: Batch adsorption studies on the removal of malachite green from water by chemically modified *Azolla pinnata*. Desalin Water Treat. doi:10.1080/19443994.2015.1065450 (2015)
9. Chieng, H.I.; Lim, L.B.L.; Priyantha, N.: Sorption characteristics of peat from Brunei Darussalam for the removal of rhodamine B dye from aqueous solution: adsorption isotherms, thermodynamics, kinetics and regeneration studies. Desalin. Water Treat. doi:10.1080/19443994.2014.919609 (2014)
10. Badii, K.; Ardejani, F.D.; Saberi, M.A.; Limaee, N.Y.; Shafaei, S.: Adsorption of Acid Blue 25 dye on diatomite in aqueous solutions. Indian J. Chem. Technol. **17**, 7–16 (2010)
11. Auta, M.; Hameed, B.H.: Preparation of waste tea activated carbon using potassium acetate as an activating agent for adsorption of Acid Blue 25 dye. Chem. Eng. J. **171**, 502–509 (2011)
12. Dahri, M.K.; Kooh, M.R.R.; Lim, L.B.L.: Water remediation using low cost adsorbent walnut shell for removal of malachite green: equilibrium, kinetics, thermodynamic and regeneration studies. J. Environ. Chem. Eng. **2**, 1434–1444 (2014)
13. Daneshvar, E.; Sohrabi, M.S.; Kousha, M.; Bhatnagar, A.; Aliakbarian, B.; Converti, A.; Norrström, A.-C.: Shrimp shell as an efficient bioadsorbent for Acid Blue 25 dye removal from aqueous solution. J. Taiwan Inst. Chem. Eng. **45**, 2926–2934 (2014)
14. Lim, L.B.L.; Priyantha, N.; Hei Ing, C.; Khairud Dahri, M.; Tennakoon, D.T.B.; Zehra, T.; Suklueng, M.: Artocarpus odoratissimus skin as a potential low-cost biosorbent for the removal of methylene blue and methyl violet 2B. Desalin. Water Treat. **53**, 964–975 (2015)
15. Priyantha, N.; Lim, L.B.L.; Dahri, M.K.: Dragon fruit skin as a potential low-cost biosorbent for the removal of manganese(II) ions. J. Appl. Sci. Environ. Sanit. **8**, 179–188 (2013)
16. Lim, L.B.L.; Priyantha, N.; Tennakoon, D.T.B.; Chieng, H.I.; Dahri, M.K.; Suklueng, M.: Breadnut peel as a highly effective low-cost biosorbent for methylene blue: Equilibrium, thermodynamic and kinetic studies. Arabian J. Chem. (2013). doi:10.1016/j.arabjc.2013.12.018
17. Chieng, H.I.; Priyantha, N.; Lim, L.B.L.: Effective adsorption of toxic brilliant green from aqueous solution using peat of Brunei Darussalam: isotherms, thermodynamics, kinetics and regeneration studies. RSC Adv. **5**, 34603–34615 (2015)
18. Huang, F.; Guo, C.-L.; Lu, G.-N.; Yi, X.-Y.; Zhu, L.-D.; Dang, Z.: Bioaccumulation characterization of cadmium by growing Bacillus cereus RC-1 and its mechanism. Chemosphere **109**, 134–142 (2014)
19. Gaur, J.P.; Noraho, N.: Adsorption and uptake of cadmium by *Azolla pinnata*: kinetics of inhibition by cations. Biomed. Environ. Sci. **8**, 149–157 (1995)
20. Rai, P.K.: Technical note: phytoremediation of Hg and Cd from industrial effluents using an aquatic free floating macrophyte *Azolla pinnata*. Int. J. Phytoremediat. **10**, 430–439 (2008)
21. Jain, S.; Vasudevan, P.; Jha, N.: *Azolla pinnata* R. Br. and Lemna minor L. for removal of lead and zinc from polluted water. Water Res. **24**, 177–183 (1990)
22. Rahman, M.A.; Hasegawa, H.: Aquatic arsenic: phytoremediation using floating macrophytes. Chemosphere **83**, 633–646 (2011)
23. Ghodbane, H.; Hamdaoui, O.: Decolorization of antraquinonic dye, C.I. Acid Blue 25, in aqueous solution by direct UV irradiation, UV/H2O2 and UV/Fe(II) processes. Chem. Eng. J. **160**, 226–231 (2010)

24. Feng, Y.; Dionysiou, D.D.; Wu, Y.; Zhou, H.; Xue, L.; He, S.; Yang, L.: Adsorption of dyestuff from aqueous solutions through oxalic acid-modified swede rape straw: adsorption process and disposal methodology of depleted bioadsorbents. Bioresour. Technol. **138**, 191–197 (2013)
25. Zehra, T.; Priyantha, N.; Lim, L.B.L.; Iqbal, E.: Sorption characteristics of peat of Brunei Darussalam V: removal of Congo red dye from aqueous solution by peat. Desalin. Water. Treat. doi:10.1080/19443994.2014.899929 (2014)
26. Lagergren, S.: Zur Theorie der Sogenannten Adsorption gel Ster Stoffe. K. Sven. Vetenskapsakad. Handl. **24**, 1–39 (1898)
27. Ho, Y.S.; McKay, G.: Pseudo-second order model for sorption processes. Process Biochem. **34**, 451–465 (1999)
28. Weber, W.; Morris, J.: Kinetics of adsorption on carbon from solution. J. Sanit. Eng. Div. **89**, 31–60 (1963)
29. Boyd, G.E.; Adamson, A.W.; M., L.S. Jr..: The exchange adsorption of ions from aqueous solutions by organic zeolites. II. Kinetics. J. Am. Chem. Soc. **69**, 2836–2848 (1947)
30. Langmuir, I.: The constitution and fundamental properties of solids and liquids. J. Am. Chem. Soc. **38**, 2221–2295 (1916)
31. Freundlich, H.M.F.: Over the adsorption in solution. J. Phys. Chem. **57**, 385–471 (1906)
32. Dubinin, M.M.; Radushkevich, L.V.: Equation of the characteristic curve of activated charcoal. Proc. Acad. Sci. **55**, 327 (1947)
33. Hanafiah, M.A.K.M.; Ngah, W.S.W.; Zolkafly, S.H.; Teong, L.C.; Majid, Z.A.A.: Acid Blue 25 adsorption on base treated Shorea dasyphylla sawdust: Kinetic, isotherm, thermodynamic and spectroscopic analysis. J. Environ. Sci. **24**, P261–268 (2012)
34. Mane, V.S.; Babu, P.: Studies on the adsorption of Brilliant Green dye from aqueous solution onto low-cost NaOH treated saw dust. Desalination **273**, 321–329 (2011)
35. Chen, H.; Zhao, J.; Dai, G.: Silkworm exuviae—a new non-conventional and low-cost adsorbent for removal of methylene blue from aqueous solutions. J. Hazard. Mater. **186**, 1320–1327 (2011)
36. Özacar, M.; Şengil, İ.A.: Application of kinetic models to the sorption of disperse dyes onto alunite. Colloids Surf. A **242**, 105–113 (2004)
37. Zhao, Y.; Yue, Q.; Li, Q.; Xu, X.; Yang, Z.; Wang, X.; Gao, B.; Yu, H.: Characterization of red mud granular adsorbent (RMGA) and its performance on phosphate removal from aqueous solution. Chem. Eng. J. **193**, 161–168 (2012)
38. Maiyalagan, T.; Karthikeyan, S.: Film-pore diffusion modeling for sorption of azo dye on to exfoliated graphitic nanoplatelets. Indian J. Chem. Technol. **20**, 7–14 (2013)
39. Rehman, M.S.U.; Munir, M.; Ashfaq, M.; Rashid, N.; Nazar, M.F.; Danish, M.; Han, J.-I.: Adsorption of Brilliant Green dye from aqueous solution onto red clay. Chem. Eng. J. **228**, 54–62 (2013)
40. Yang, Y.; Jin, D.; Wang, G.; Liu, D.; Jia, X.; Zhao, Y.: Biosorption of Acid Blue 25 by unmodified and CPC-modified biomass of Penicillium YW01: kinetic study, equilibrium isotherm and FTIR analysis. Colloids Surf. B Biointerfaces **88**, 521–526 (2011)
41. Ruixia, W.; Jinlong, C.; Lianlong, C.; Zheng-hao, F.; Ai-min, L.; Quanxing, Z.: Study of adsorption of lipoic acid on three types of resin. React. Funct. Polym. **59**, 243–252 (2004)
42. Keeler, J.; Wothers, P.: Why Chemical Reactions Happen. Oxford University Press, Oxford (2003)